



HAL
open science

Dislocation patterning and deformation processes in ice single crystals deformed by torsion

Juliette Chevy, Maurine Montagnat, Paul Duval, Marc C. Fivel, Jerome Weiss

► **To cite this version:**

Juliette Chevy, Maurine Montagnat, Paul Duval, Marc C. Fivel, Jerome Weiss. Dislocation patterning and deformation processes in ice single crystals deformed by torsion. *Physics and Chemistry of Ice*, Jul 2006, Bremerhaven Germany. hal-01698729

HAL Id: hal-01698729

<https://hal.science/hal-01698729>

Submitted on 2 Feb 2018

HAL is a multi-disciplinary open access archive for the deposit and dissemination of scientific research documents, whether they are published or not. The documents may come from teaching and research institutions in France or abroad, or from public or private research centers.

L'archive ouverte pluridisciplinaire **HAL**, est destinée au dépôt et à la diffusion de documents scientifiques de niveau recherche, publiés ou non, émanant des établissements d'enseignement et de recherche français ou étrangers, des laboratoires publics ou privés.

DISLOCATION PATTERNING AND DEFORMATION PROCESSES IN ICE SINGLE CRYSTALS DEFORMED BY TORSION

J. Chevy^{1,2}, M. Montagnat¹, P. Duval¹, M. Fivel² and J. Weiss¹

¹Laboratoire de Glaciologie et Géophysique de l'Environnement, 38402 St Martin d'Hères, France.

²Génie Physique et Mécanique des Matériaux, ENSPG, 101 Rue de la Physique, BP 46, 38402 St Martin d'Hères, France.

1 INTRODUCTION

The early observation of macroscopic “slip lines” in deformed ice single crystals by Nakaya (1958)¹ or Readings and Bartlett (1968)² indicated the simultaneous and correlated motion of many dislocations. More recently, acoustic emission analyses performed on ice single crystals during deformation³ revealed the scale-free intermittent motion of dislocations through dislocation avalanches.

In this paper we present synchrotron X-ray analysis of ice single crystals deformed in pure torsion. The observation of diffraction topographs revealed scale invariant arrangement of dislocations, independently of the macroscopically imposed deformation gradient⁴. Scale invariant patterning is thought to be induced by the long-range interactions between dislocations. This spatio-temporal heterogeneity of slip is induced by the motion of dislocations in a collective and self organized manner that can not be described in terms of local and uncorrelated relaxations of individual dislocation segments toward configurations of lower energy⁵.

Preliminary Dislocation Dynamics (DD) simulations using the model developed by Verdier *et al.*⁶ provide a plausible scenario for the dislocation patterning occurring during the deformation of ice single crystals based on cross-slip mechanism. The simulated dislocation multiplication mechanism is consistent with the scale invariant patternings observed experimentally.

2 EXPERIMENTAL OBSERVATIONS

2.1 Torsion deformation of ice single crystals

Pure torsion tests were performed on ice single crystals at a constant imposed external shear stress^{4,7}. Softening was evidenced as the creep curves revealed a strain-rate increase, up to a cumulated plastic strain of 7%, see figure 1. Note that such a behaviour was also observed during compression and tension tests^{8,9}.

The initial dislocation density of the sample was estimated to be less than 10^8 m^{-2} . The orientation of the samples was chosen in order to align the torsion axis as close as possible with the c-axis ($\pm 1^\circ$). The maximum resolved shear stress is then applied on the basal planes. The plastic deformation is accommodated by the glide of screw dislocations on the

three slip systems $a/3\langle 11-20 \rangle \{0001\}$ contained within the basal planes. We assume that dislocations can be freely nucleated at the surface of the sample, where the imposed shear stress is the highest.

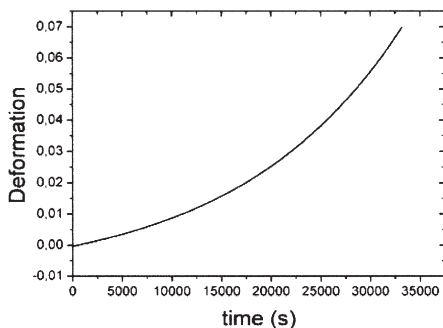


Figure 1 Typical creep curve of an ice single crystal deformed in torsion up to 7% along the c -axis. The deformation is the measured shear strain on the surface.

2.2 X-ray diffraction analyses

Specimens were extracted from the deformed samples at different radii from the cylinder axis, along the torsion axis direction. Some of the diffraction analyses were performed using a hard X-ray diffraction technique developed at Institut Laue Langevin, others were observed via synchrotron X-ray diffraction topography at ESRF (European Synchrotron Radiation Facilities) on the "ID19" beamline.

The hard-ray diffraction technique allows a fast characterization of the lattice distortions for sample size in the centimeter range or more¹⁰. The spatial resolution is low, but this technique showed the predominance of excess screw dislocations to accommodate the torsion deformation in all deformed crystals⁷. A negligible contribution of edge dislocations was evidenced, which is consistent with the loading conditions.

The ID19 beamline at ESRF is characterized by a spectrally and spatially homogeneous, highly coherent beam at the sample position. X-ray topography, an imaging technique based on Bragg diffraction, provides a two-dimensional intensity mapping of the beam(s) diffracted by the crystal. Topography analysis consists in the study of the fine structure of a Bragg spot which contains all the information about the defect structure. High energy (50-120 keV) white beam (with all wavelengths in the provided energy range) was used to allow the investigation of bulk ice samples in transmission⁴. Final images provide a final resolution of about 10 μ m. The topograph given in figure 2 is the diffraction pattern on the prismatic plane for a specimen extracted from a sample deformed at 2.69%.

The diffracted intensity records the orientation contrast and is, in our case, related to the dislocation density at the origin of the lattice distortion⁴. Although a direct relationship between diffracted intensity variations and dislocation density is difficult to assess, darker zones in the topographs correspond to higher dislocation density regions. We extracted the dislocation density variation signal along 1D profiles in the direction of the c -axis (figure 2) on [100] prismatic plane diffraction pattern. Indeed, as no extinction is expected for any of the 3 glide systems with $a/3\langle 11-20 \rangle$ Burgers vectors, the signal on this diffraction pattern is supposed to be complete.

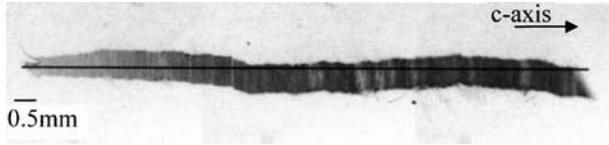


Figure 2 Diffraction pattern on the prismatic plane for a specimen taken from a sample deformed at 2.69%. The long dimension is the height of the specimen, while the width corresponds to the size of the diffracted beam through 0.1mm slit. The intensity profile is taken along the black line.

Spectral analyses were performed along the 1D intensity profiles. The scaling properties of the profiles are independent on the position of the profile along the basal plane. The diffracted intensity along the 1D profile is spatially heterogeneous in the sense that it is not distributed around a mean value following a Gaussian distribution; instead it is characterized by a wide distribution and, as shown below, by spatial correlations. Figure 3 shows the power spectrum of the intensity record taken along a profile as represented in figure 2 (calculated from the fast Fourier transform of the signal). The power spectrum is characterized by a power law regime over the entire available scale range (bounded by the resolution of the analysis, and by the sample size), $E(f) \sim f^{-\mu}$. These scale ranges extend over more than 2 orders of magnitude, from 15 μm to about 7 mm. The power spectra obtained on 2 samples deformed at different levels are characterized by a same exponent $\mu=1.3\pm 0.1$. Such a power law reveals the scale invariance of the intensity records.

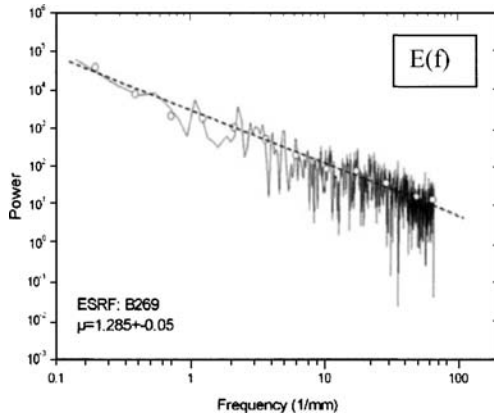


Figure 3 Power spectrum of the intensity record taken from a 1D profile along the topograph represented in figure 2.

Such scale invariant spectra reveal that the dislocation density variation is scale invariant, and put forward spatial correlations over very large distances with a correlation length of the order of the system (sample) size³. This is confirmed with the autocorrelation function of the records shown in figure 4, in which is also represented a signal taken from a

non-deformed sample. The autocorrelation function obtained for the deformed sample slowly decreases with increasing distance Δx , to fall around nil values for distances of few millimetres, whereas the correlation falls off for much lower distances on the non-deformed sample. The increase in long-range correlations is due to the deformation processes. Such correlations are the fingerprints of strong interactions between dislocations. Thus, dislocations are neither distributed randomly, nor concentrated on well-defined “slip bands” more or less regularly spaced. Instead, they self-organize into a scale free pattern.

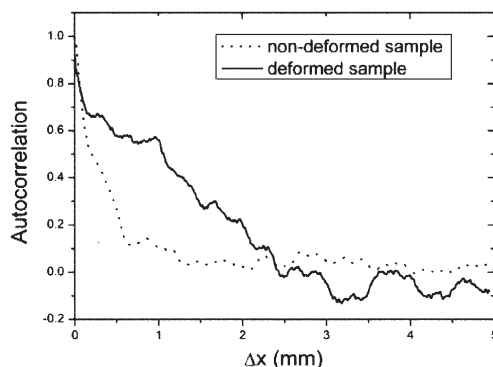


Figure 4 Autocorrelation functions obtained for a deformed sample and a non-deformed sample.

3 DISLOCATION DYNAMICS SIMULATIONS. Preliminary results

The Discrete Dislocation Dynamics code used here is based on the discretization of dislocations into edge and screw segments whose extremities are located on the nodes of a discrete network. Each dislocation segment displacement is due to an effective stress, which depends on the applied stress, the internal stress and the Peierls lattice friction. Cross-slip is allowed for the screw component of a dislocation line through a probabilistic law which involves the resolved shear stress in the deviate system. The code was originally developed for FCC metals⁶. In this study, it has been adapted to the simulation of the torsion deformation of ice single crystals mainly by selecting 3 over the 12 FCC glide systems to represent the ice slip systems (hexagonal symmetry). The torsion moment is applied through a shear stress proportional to the radius superimposed to the internal stress fields. Dislocations sources are randomly spread at the outer radius of the specimen, where the applied shear stress induced by the moment is the highest.

When a moment is applied along the c-axis, screw dislocations are simultaneously activated in the 3 coplanar basal glide systems $\langle 11-20 \rangle \{0001\}$. These dislocations are pushed toward the torsion axis inducing a kind of pile up in each glide system. Although the torsion loading does not induce any applied stress in the prismatic system, the internal stresses due to the dislocation arrangement create a shear stress component on the prismatic system that could favour cross slip events. Thus, when the shear stress component is higher in the prismatic plane than in the basal plane, a screw dislocation has a high probability to cross slip under the internal driving force. Then, at a given distance from the initial basal plane, the shear stress in the prismatic plane becomes lower than that

of the basal plane and the dislocation cross slip back to the primary system. Such a double cross-slip creates a Koehler source that emits basal dislocations in a new basal plane.

Figure 5 represents a typical evolution of the dislocation pattern during the deformation. The simulation was performed in a 20 mm diameter crystal, with 2 initial basal planes activated (one system in each plane) at the beginning of the deformation. It clearly appears that the double cross-slip mechanism propagates the plasticity in many other basal planes. One can also notice the asymmetry in the plane expansion due to the dislocation interactions.

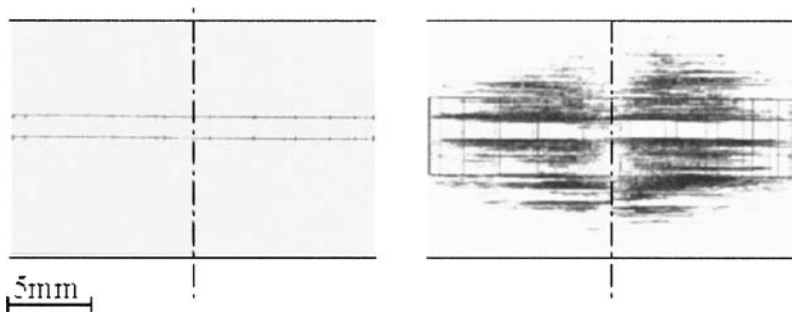


Figure 5 Thickening of slip planes due to the double cross-slip of basal dislocations. Beginning of the simulation (left), after deformation (right). Basal dislocations glide horizontally (horizontal lines), dislocations in the prismatic plane vertically (white vertical lines). The center of the cylinder is represented.

4 DISCUSSION

During the torsion experiments performed in this study, only screw dislocations are activated on the basal planes by the imposed shear stress. If dislocations can easily nucleate at the free surface, such a random multiplication process cannot explain the spatial correlations observed by X-Ray diffraction topography. As suggested by the DD modelling, the double cross-slip mechanism appears to be an efficient mechanism to provide a dislocation multiplication process that strongly depends on neighbouring dislocation interactions. As previously modeled by Mendelson¹¹, cross-slip is enhanced by the repulsive stress of neighbouring screw arrays. Such a propagation of dislocation slip in other planes is influenced by dislocation interactions, and can lead to scale invariant patterning for dislocation arrangements with long range correlations.

The double cross-slip mechanism can then be considered as the most probable deformation process, complementary to the basal slip. Indeed, dislocation climb can hardly be invoked in this torsion loading conditions since most of the dislocations are of screw type.

Usually, creep deformation of ice single crystals is associated to a steady-state creep regime, with a stress exponent equal to 2 when basal glide is activated^{8,9}. In the torsion experiments performed, the steady-state creep was not reached, but one would expect it to be achieved for larger strain when the immobilisation of the basal dislocations in the pile-ups is balanced by the dislocation multiplication induced by the double cross-slip mechanism.

In summary, torsion creep tests on well-oriented ice single crystals appear to be a pertinent experiment to try to understand and represent the fundamental mechanisms of deformation in ice single crystals. The presented evidence for the occurrence of cross-slip as a rate-limiting process questions the role of dislocation climb as suggested by Louchet (2004)¹².

References

- 1 U. Nakaya, in Mechanical properties of single crystals of ice (US Army Snow Ice and Permafrost Res. Establish 1958) Report 28, 1958.
- 2 C.J. Readings and J.T. Bartlett, *J. Glaciol.*, 1968, **51**, 479.
- 3 J. Weiss and J.R. Grasso, *J. Phys. Chem.*, 1997, **101**, 6113-6117.
- 4 M. Montagnat, J. Weiss, J. Chevy, P. Duval, H. Brunjail, P. Bastie and J. Gil Sevillano, *Phil. Mag.*, 2006, **86**, 4259.
- 5 H. Neuhauser, in Dislocations in Solids, edited by F.R.N. Nabarro (North Holland, Amsterdam 1983) pp. 319.
- 6 M. Verdier, M. Fivel and I. Groma, *Mod. Simul. Mater. Sci. Eng.*, 1998, **6**, 755.
- 7 M. Montagnat, P. Duval, P. Bastie, B. Hamelin, *Scripta Mater.*, 2003, **49**, 411.
- 8 S.J. Jones and J.W. Glen, *J. Glaciol.*, 1969, **8**, 463.
- 9 A. Higashi, S. Koinuma and S. Mae, *Japanese J. Appl. Phys.*, 1964, **3**, 610.
- 10 B. Hamelin and P. Bastie, *J. Phys. IV France*, 2004, **118**, 27.
- 11 S. Mendelson, *Phil. Mag.*, 1963, **8**, 1633.
- 12 F. Louchet, *Phil. Mag. Let.*, 2004, **84**, 797.